

1 **Natural variation in fertility is correlated with species-wide levels of divergence in**

2 ***Caenorhabditis elegans***

3

4 **Gaotian Zhang\*, Jake D. Mostad\*, Erik C. Andersen\*,<sup>1</sup>**

5

6 \*Molecular Biosciences, Northwestern University, Evanston, IL 60208

7

8 ORCID IDs: 0000-0001-6468-1341 (G.Z.); 0000-0003-0229-9651 (E.C.A.)

9

10 <sup>1</sup>Corresponding author:

11 Erik C. Andersen

12 Department of Molecular Biosciences

13 Northwestern University

14 4619 Silverman Hall

15 2205 Tech Drive

16 Evanston, IL 60208

17 E-mail: [erik.andersen@northwestern.edu](mailto:erik.andersen@northwestern.edu)

18

19 **KEYWORDS**

20 *C. elegans*, Lifetime fertility, Natural variation, QTL, Selective sweeps

21

22

23

## 24 ABSTRACT

25 Life history traits underlie the fitness of organisms and are under strong natural selection  
26 in the face of environmental challenges. A new mutation that positively impacts a life  
27 history trait will likely increase in frequency and become fixed in a population (e.g.  
28 selective sweep). The identification of the beneficial alleles that underlie selective sweeps  
29 provides insights into the mechanisms that occurred during the evolution of species. In  
30 the global population of *Caenorhabditis elegans*, we previously identified selective  
31 sweeps that have drastically reduced chromosomal-scale genetic diversity in the species.  
32 Here, we measured the fertility (viable offspring) of a collection of wild *C. elegans* strains,  
33 including many recently isolated divergent strains from the Hawaiian islands and found  
34 that strains with larger swept genomic regions on multiple chromosomes have  
35 significantly higher fertility than strains that do not have evidence of the recent selective  
36 sweeps. We used genome-wide association (GWA) mapping to identify three quantitative  
37 trait loci (QTL) underlying the fertility variation. Additionally, we mapped previous fertility  
38 data of wild *C. elegans* strains and *C. elegans* recombinant inbred advanced intercross  
39 lines (RIAILs) that were grown in various conditions and detected eight QTL across the  
40 genome using GWA and linkage mappings. These QTL show the genetic complexity of  
41 life history traits such as fertility across this species. Moreover, the haplotype structure in  
42 each GWA QTL region revealed correlations with recent selective sweeps in the *C.*  
43 *elegans* population. North American and European strains had significantly higher fertility  
44 than most strains from Hawaii, a hypothesized origin of the *C. elegans* species,  
45 suggesting that beneficial alleles that cause increased fertility could underlie the selective  
46 sweeps during the worldwide expansion of *C. elegans*.

47 **INTRODUCTION**

48 Life history traits are phenotypic characters that affect the fitness of organisms (Knight  
49 and Robertson 1957; Stearns 1976, 1989; Charlesworth *et al.* 2003; Flatt and Heyland  
50 2011; Flatt 2020). Traits, such as fertility, size at birth, age at reproductive maturity, and  
51 stage- or size- specific rates of survival, interact with each other to affect the fitness of  
52 organisms in an ever-changing environment. Genes that affect life history traits should be  
53 subject to strong natural selection because they directly affect the fitness of organisms.  
54 Adaptive alleles with strong selective advantages in life history related genes are likely to  
55 spread rapidly across a population in a selective sweep (Smith and Haigh 1974; Kaplan  
56 *et al.* 1989; Berry *et al.* 1991; Stephan 2019). Signatures of selective sweeps include a  
57 loss of neutral polymorphism, drastic changes in the site frequency spectrum, and  
58 particular patterns of linkage disequilibrium (LD) across the site of selection (Smith and  
59 Haigh 1974; Braverman *et al.* 1995; Fay and Wu 2000; Kim and Nielsen 2004; Stephan  
60 *et al.* 2006; Stephan 2019). Identification of selective sweeps by these signatures  
61 provides a key to locate genes under selection and helps to understand the process of  
62 adaptation and evolution.

63 *Caenorhabditis elegans* is a free-living nematode and a keystone model organism  
64 for biological research. The reproductive mode of *C. elegans* is androdioecy, with  
65 predominant self-fertilization of hermaphrodites and rare outcrossing between  
66 hermaphrodites and males (Brenner 1974). A single hermaphrodite of the laboratory  
67 reference strain N2 lays approximately 300 self-fertilized embryos in standard laboratory  
68 conditions (Hodgkin and Doniach 1997; Félix and Braendle 2010). Newly hatched animals  
69 develop through four larval stages (L1 to L4) into mature reproductive adults after three

70 days in favorable conditions at 20°C (Frézal and Félix 2015). Under stressful conditions,  
71 such as crowding and limited food, *C. elegans* enters the dauer diapause stage during  
72 larval development to enable survival in harsh environments and to facilitate dispersal. *C.*  
73 *elegans* likely has a boom-and-bust life cycle in the wild because of fluctuating  
74 environmental conditions and the spatio-temporal distributed habitats, such as rotting  
75 fruits and stems (Félix and Duveau 2012; Frézal and Félix 2015). *C. elegans* is globally  
76 distributed (Kiontke *et al.* 2011; Andersen *et al.* 2012; Félix and Duveau 2012; Cook *et*  
77 *al.* 2017; Crombie *et al.* 2019; Lee *et al.* 2020). Although recent studies characterized  
78 high genetic diversity of the species in Hawaii and the surrounding Pacific regions  
79 (Crombie *et al.* 2019; Lee *et al.* 2020), *C. elegans* exhibits low overall genetic diversity at  
80 the global scale (Barrière and Félix 2005; Cutter 2006; Andersen *et al.* 2012). The  
81 metapopulation dynamics, seasonal bottlenecks, predominant selfing, low outcrossing  
82 rate, low recombination rate, background selection, and recent selective sweeps might  
83 all contribute to the low genetic diversity of the species (Barrière and Félix 2005, 2007;  
84 Cutter 2006; Rockman and Kruglyak 2009; Rockman *et al.* 2010; Andersen *et al.* 2012).  
85 In the genomes of many *C. elegans* strains sampled in temperate regions, chromosomes  
86 I, IV, V, and X exhibit signatures of selective sweeps, such as an excess of rare variants,  
87 high linkage disequilibrium (LD), and extended haplotype homozygosity over large  
88 genomic regions (Andersen *et al.* 2012). By contrast, the genomes of most Hawaiian *C.*  
89 *elegans* strains have no such signatures (Andersen *et al.* 2012; Crombie *et al.* 2019; Lee  
90 *et al.* 2020). Analyses of *C. elegans* genetic diversity, population structure, gene flow, and  
91 haplotype structure suggest that *C. elegans* originated from the Pacific region, such as  
92 the Hawaii Islands, the western United States, or New Zealand, and expanded worldwide,

93 especially into human-associated habitats (Andersen *et al.* 2012; Crombie *et al.* 2019;  
94 Lee *et al.* 2020). The recent positive selective sweeps likely occurred during this  
95 expansion, but the beneficial alleles that have driven the sweeps and their fitness  
96 advantages are yet unknown.

97 Here, we measured lifetime fertility of 121 wild *C. elegans* strains and compared  
98 this trait between swept strains that experienced the recent selective sweeps and  
99 divergent strains that avoided these sweeps. We found that swept strains had significantly  
100 higher lifetime fertility than divergent strains, as well as significant geographical  
101 differences in lifetime fertility between strains from the Hawaii Islands and strains from  
102 other parts of the world. We then used GWA mapping to identify three QTL on  
103 chromosome I, II, and V that influence the lifetime fertility of *C. elegans*. Additionally, we  
104 identified eight QTL impacting *C. elegans* fertility in different environments using GWA  
105 and linkage mappings of previous fertility data. The 11 QTL reveal the complex genetic  
106 architecture of *C. elegans* fertility. Furthermore, we discovered that the different alleles at  
107 each QTL peak marker and the different haplotypes in each QTL among the 121 strains  
108 were strongly correlated with signatures of recent selective sweeps found in each strain.  
109 Our results suggest that higher lifetime fertility could have provided selective advantages  
110 for swept strains and the underlying genetic variants might have driven the recent strong  
111 sweeps in the *C. elegans* strains that have colonized the world.

112

## 113 MATERIALS AND METHODS

### 114 *C. elegans* strains

115 All the wild strains were obtained from *C. elegans* Natural Diversity Resource (CeNDR)  
116 (Cook *et al.* 2017). Animals were cultured at 20°C on modified nematode growth medium  
117 (NGMA) containing 1% agar and 0.7% agarose to prevent burrowing and fed *Escherichia*  
118 *coli* (*E. coli*) strain OP50. Prior to each assay, strains were grown for three generations  
119 without entering starvation or encountering dauer-inducing conditions (Andersen *et al.*  
120 2014).

121

## 122 **Swept haplotypes and strains**

123 Haplotype data for 403 *C. elegans* isotypes, representing 913 wild strains, were acquired  
124 from the 20200815 CeNDR release. We compared the total length of each haplotype per  
125 chromosome across all isotypes to identify the most common haplotypes on each  
126 chromosome. We then searched for the regions of the most common haplotypes in each  
127 *C. elegans* isotype and recorded them if their length was greater than 1 Mb (Crombie *et*  
128 *al.* 2019; Lee *et al.* 2020). We classified haplotypes outside of recorded regions as  
129 unswept haplotypes. The swept status of some haplotypes was undetermined when no  
130 identical-by-descent groups were found, and thus the haplotype information for that  
131 region was missing in the CeNDR release.

132 Signatures of selective sweeps were identified on chromosomes I, IV, V, and X,  
133 but not on chromosomes II and III (Andersen *et al.* 2012). Therefore, we focused on the  
134 four chromosomes (I, IV, V, and X) and defined their most common haplotypes as swept  
135 haplotypes (Lee *et al.* 2020). In each *C. elegans* isotype, chromosomes that contain  
136 greater than or equal to 30% of the swept haplotype were classified as swept  
137 chromosomes. We classified isotypes with any swept I, IV, V, and X chromosomes as

138 swept isotypes and isotypes without any swept I, IV, V, and X chromosomes as divergent  
139 isotypes. Strains that belong to swept isotypes and divergent isotypes were classified as  
140 swept strains and divergent strains, respectively (Gilbert *et al.* 2020).

141

#### 142 **Genetic relatedness**

143 Genetic variation data for 403 *C. elegans* isotypes were acquired from the hard-filtered  
144 isotype variant call format (VCF) 20200815 CeNDR release. These variants were pruned  
145 to the 1,074,596 biallelic single nucleotide variants (SNVs) without missing genotypes.  
146 We converted this pruned VCF file to a PHYLIP file using the vcf2phylip.py script (Ortiz  
147 2019). The unrooted neighbor-joining tree was made using the R packages phangorn  
148 (v2.5.5) and ggtree (v1.14.6) (Schliep 2011; Yu *et al.* 2017).

149

#### 150 **Fertility measurements**

151 For each *C. elegans* strain, single L4 larval stage hermaphrodites were picked to each of  
152 five 3.5 cm plates with NGMA and OP50, and were maintained at 20°C. For each assay  
153 plate, the original hermaphrodite parent was transferred to a fresh plate every 24 hours  
154 for 96 hours. A custom-built imaging platform (DMK 23GP031 camera; Imaging Source,  
155 Charlotte, NC) was used to collect images for each of the first four assay plates (0, 24,  
156 48, and 72 hour samples) 48 hours after removal of the parent from each plate. Most  
157 strains had few offspring after 96 hours. Images of the fifth assay plates were collected  
158 72 hours after the final transfer of the parents. From each image, the total offspring was  
159 counted by visual inspection using the Multi-point Tool in ImageJ (v1.8.0\_162) (Schneider  
160 *et al.* 2012). The original hermaphrodite parents on the fifth assay plates were excluded

161 from the counts. The number of offspring in each of the first four assay plates corresponds  
162 to the daily fertility. Numbers of offspring on the fifth assay plates contained offspring from  
163 three days. For each biological replicate of each *C. elegans* strain, the lifetime fertility was  
164 calculated as the total number of offspring from the five plates. Few parent animals died  
165 during the assays. Only biological replicates with data from all five assay plates were used  
166 in the calculations of daily and total fertility. We collected fertility data for 557 replicates  
167 of 121 *C. elegans* strains (mean lifetime fertility (MLF) = 231, standard deviations (SD) =  
168 55): 84 strains with five replicates (MLF = 232, SD = 55), 28 strains with four replicates  
169 (MLF = 229, SD = 52), seven strains with three replicates (MLF = 214, SD = 49), and two  
170 strains with two replicates (MLF = 292, SD = 19).

171

## 172 **Genome-wide association (GWA) mapping**

173 GWA mapping was performed on the mean fertility measurements of biological replicates  
174 from 121 *C. elegans* strains, which belong to 121 distinct isotypes. Genotype data for  
175 each of the 121 isotypes were acquired from the hard-filtered isotype VCF (20200815  
176 CeNDR release). We performed the mapping using the pipeline cegwas2-nf  
177 (<https://github.com/AndersenLab/cegwas2-nf>) as previously described (Zdraljevic *et al.*  
178 2019; Na *et al.* 2020). Briefly, we used BCFtools (Li 2011) to filter variants that had any  
179 missing genotype calls and variants that were below the 5% minor allele frequency. We  
180 used PLINK v1.9 (Purcell *et al.* 2007; Chang *et al.* 2015) to prune the genotypes to 56,878  
181 markers with a linkage disequilibrium (LD) threshold of  $r^2 < 0.8$  and then generated the  
182 kinship matrix using the *A.mat* function in the R package rrBLUP (v4.6.1) (Endelman  
183 2011). The number of independent tests ( $N_{test}$ ) within the genotype matrix was estimated

184 using the R package RSpectra (v0.16.0) (<https://github.com/yixuan/RSpectra>) and  
185 correlateR (0.1) (<https://github.com/AEBilgrau/correlateR>). The eigen-decomposition  
186 significance (EIGEN) threshold was calculated as  $-\log_{10}(0.05/N_{test})$ . We used the GWAS  
187 function in the rrBLUP package to perform the genome-wide mapping with the EMMA  
188 algorithm (Kang *et al.* 2008). QTL were defined by at least one marker that was above  
189 the Bonferroni-corrected significance (BF) threshold, to locate the best estimate of QTL  
190 positions with the highest significance. We used the LD function from the R package  
191 genetics (v1.3.8.1.2) (<https://cran.r-project.org/package=genetics>) to calculate the LD  
192 correlation coefficient  $r^2$  among the QTL peak markers associated with *C. elegans* lifetime  
193 fertility.

194 We also performed GWA mapping using fertility data in DMSO control conditions  
195 from a previous study (Hahnel *et al.* 2018), where 236 *C. elegans* wild strains were  
196 cultured and phenotyped using the high-throughput fitness assays (HTA) as previously  
197 described. Briefly, L4 larval stage hermaphrodites were cultured to gravid adult stage on  
198 plates and were bleached to obtain synchronized offspring. The embryos were grown to  
199 L4 larval stage in liquid (K medium) (Boyd *et al.* 2012) and fed an *E. coli* HB101 lysate  
200 (García-González *et al.* 2017) in 96-well plates. A large-particle flow cytometer (COPAS  
201 BIOSORT; Union Biometrica, Holliston, MA) was used to sort three L4 larvae into each  
202 well of new 96-well plates containing K medium, *E. coli* HB101 lysate, and 1% DMSO.  
203 Animals in the 96-well plates were incubated at 20°C for 96 hours to allow animals to  
204 grow and produce offspring, followed by measurements of various fitness parameters,  
205 including fertility. Raw fertility data were pruned, normalized, and regressed using the R

206 package *easysorter* (v1.0) (Shimko and Andersen 2014; Hahnel *et al.* 2018). The  
207 processed fertility, norm.n, of each strain was used here for GWA mapping.

208

## 209 **Statistical analysis**

210 Statistical significance of fertility differences between swept strains (groups) and  
211 divergent strains (groups), and fertility differences among different sampling locations,  
212 was tested with the Wilcoxon test using the *stat\_compare\_means* function in the R  
213 package *ggpubr* (v0.2.4) (<https://github.com/kassambara/ggpubr/>). Broad-sense  
214 heritability of *C. elegans* lifetime fertility was calculated using the *lmer* function in the R  
215 package *lme4* (v1.1.21) with the model *phenotype ~ 1 + (1|strain)* (Bates *et al.* 2015).

216

## 217 **Linkage mapping**

218 We performed linkage mapping using fertility data from a large panel of recombinant  
219 inbred advanced intercross lines (RIAILs) derived from QX1430 and CB4856 (Andersen  
220 *et al.* 2015). The fertilities (norm.n) of the RIAILs and the parents were measured using  
221 the HTA as described above, under three conditions: 1% H<sub>2</sub>O (402 RIAILs), 1% DMSO  
222 (417 RIAILs), and 0.5% DMSO (432 RIAILs). Linkage mapping was performed on each  
223 trait using the R package *linkagemapping* (v1.3)  
224 (<https://github.com/AndersenLab/linkagemapping>) and the single-nucleotide variation  
225 data of the RIAILs in the package as described previously (Evans and Andersen 2020).  
226 Briefly, logarithm of the odds (LOD) scores for each genetic marker and each trait were  
227 calculated using the function *fsearch*. The QTL threshold for significant LOD scores in  
228 each mapping was defined by permuting trait values 1000 times, mapping the permuted

229 trait data, and taking the 95th quantile LOD score as the 5% genome-wide error rate. 95%  
230 confidence intervals of each QTL were determined using the function *annotate\_lods*.

231

## 232 **Data availability**

233 File S1 contains the haplotype data of 403 *C. elegans* isolates from CeNDR release  
234 20200815. File S2 contains genetic relatedness of 403 *C. elegans* isolates. File S3  
235 contains lifetime fertility of 121 *C. elegans* strains and their classification of swept strains  
236 and divergent strains. File S4 contains daily fertility of 121 *C. elegans* strains. File S5  
237 contains GWA results on lifetime fertility of 121 *C. elegans* strains. File S6 contains  
238 genotype and phenotype data of 121 *C. elegans* strains at the peak markers of GWA  
239 mapping. File S7 contains the sampling locations of 121 *C. elegans* strains. File S8  
240 contains the GPS coordinates of sampling locations of 121 *C. elegans* strains. File S9  
241 contains lifetime fertility and swept and divergent classifications of each of the four swept  
242 chromosomes for each of the 121 *C. elegans* strains. File S10 contains LD results among  
243 the three QTL of GWA using 121 *C. elegans* strains. File S11 contains the shared  
244 haplotypes of the 121 strains within the QTL of GWA mapping. File S12 contains GWA  
245 results on fertility data of 236 strains from a previous study (Hahnel *et al.* 2018). File S13  
246 contains genotype and phenotype data of 236 strains at the peak marker of GWA  
247 mapping. File S14 contains the shared haplotypes of the 236 strains within the QTL of  
248 GWA mapping. File S15 contains the linkage mapping results for the 402 RIAILs in 1%  
249 water condition. File S16 contains genotype and phenotype data of the 402 RIAILs at the  
250 peak markers and phenotype data of the parents in linkage mapping results. File S17  
251 contains the linkage mapping results for the 417 RIAILs in 1% DMSO condition. File S18

252 contains genotype and phenotype data of the 417 RIAILs at the peak markers and  
253 phenotype data of the parents in linkage mapping results. File S19 contains the linkage  
254 mapping results for the 432 RIAILs in 0.5% DMSO condition. File S20 contains genotype  
255 and phenotype data of the 432 RIAILs at the peak markers and phenotype data of the  
256 parents in linkage mapping results. The datasets and code for generating figures can be  
257 found at [https://github.com/AndersenLab/swept\\_broods](https://github.com/AndersenLab/swept_broods).

258

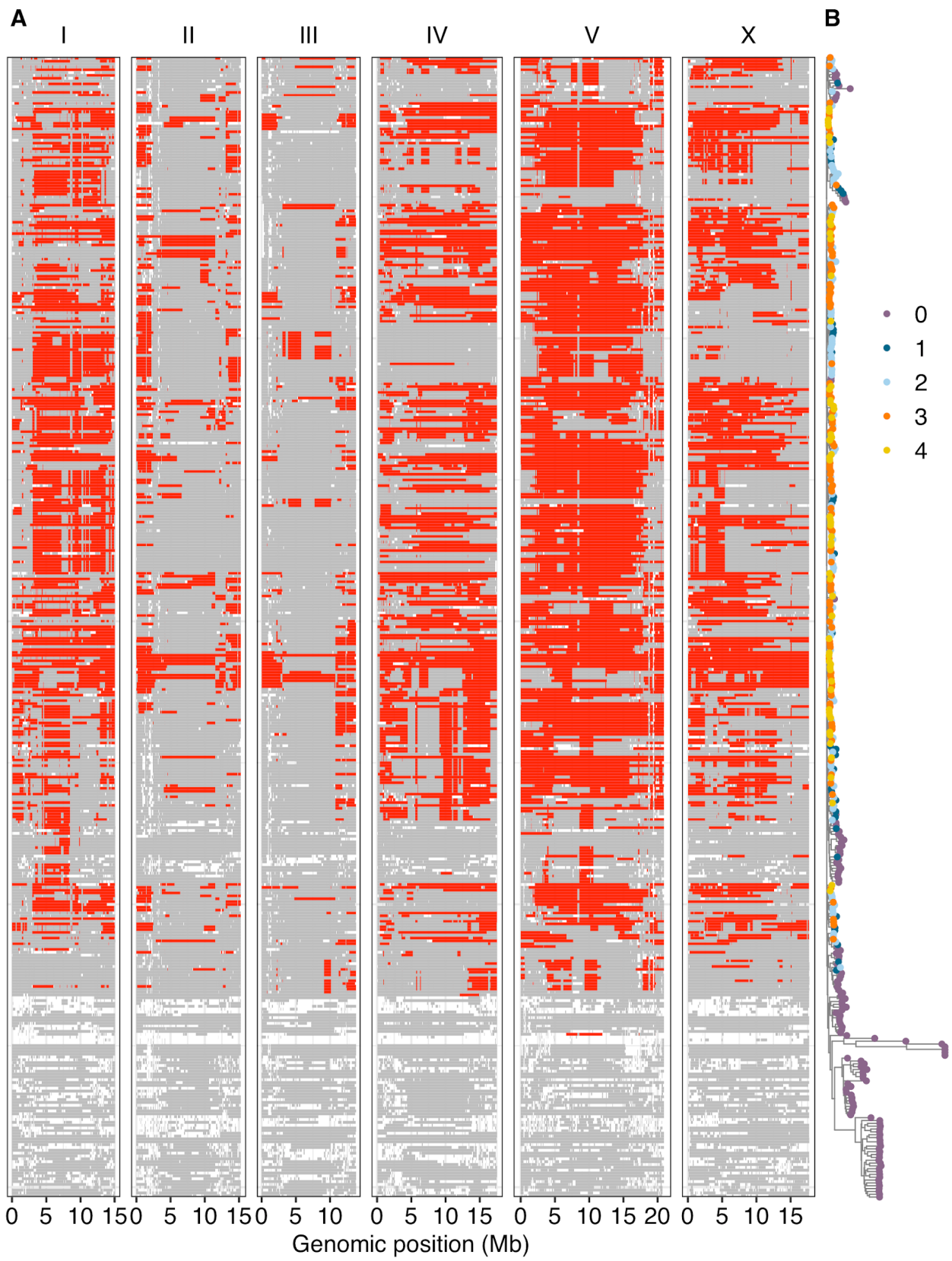
259 **RESULTS**

260 **Chromosome-scale sweeps shape *C. elegans* strain relationships**

261 Genomic information of 913 wild *C. elegans* strains, grouped into 403 genetically distinct  
262 isotypes, are currently available in *C. elegans* Natural Diversity Resource (CeNDR) (Cook  
263 *et al.* 2017). The latest CeNDR haplotype data, inferred from identical-by-descent groups  
264 among the 403 isotypes, include 22,859 distinct haplotypes across the genome. The  
265 number of haplotypes on each chromosome ranged from 2,567 to 5,199. We identified  
266 11 most common haplotypes found in the majority of wild strains. Of the 403 *C. elegans*  
267 isotypes, 331 share more than 1 Mb of regions with at least one of the 11 most common  
268 haplotypes, particularly on chromosomes I, IV, V and X (Figure 1A, File S1). The  
269 haplotype structure of shared haplotypes over large regions across 403 isotypes further  
270 supported the selective sweeps identified previously (Andersen *et al.* 2012).

271 The shared fraction of the most common haplotypes per chromosome varies in  
272 each *C. elegans* isotype. Among chromosomes with shared regions in the 331 isotypes,  
273 chromosomes I, II, III, IV, V and X have mean shared fractions and SD of  $0.45 \pm 0.25$ ,  
274  $0.21 \pm 0.19$ ,  $0.22 \pm 0.17$ ,  $0.52 \pm 0.28$ ,  $0.60 \pm 0.27$ , and  $0.43 \pm 0.28$ , respectively. We

275 focused on swept haplotypes, the most common haplotypes on chromosomes I, IV, V  
276 and X, where evidence of selective sweeps were identified (Andersen *et al.* 2012). The  
277 chromosomal sharing of swept haplotypes contributes substantially to the genetic  
278 relatedness of *C. elegans* isotypes (Figure 1B, File S2). Isotypes with swept  
279 chromosomes, which contain greater than or equal to 30% of swept haplotypes, clustered  
280 together. Of the 331 isotypes noted above, 281 have at least one swept chromosome  
281 (Figure 1B). We classified these 281 *C. elegans* isotypes as swept isotypes. We found  
282 that 244 swept isotypes have at least two swept chromosomes. By contrast, most of the  
283 122 divergent isotypes with no swept chromosomes clustered together (Figure 1B).  
284 Previous analyses on genome-wide average nucleotide diversity ( $\pi$ ), Tajima's  $D$ , and  
285 genome-wide Hudson's  $F_{st}$  between 43 Hawaiian isotypes (most are divergent isotypes)  
286 and 233 non-Hawaiian isotypes (most are swept isotypes) also revealed a high degree of  
287 divergence, the highest of which were found in genomic regions impacted by the selective  
288 sweeps (Crombie *et al.* 2019). The high degree of genetic relatedness across the species  
289 is driven by the selective sweeps, but the fitness advantage causing the strong selective  
290 sweeps is yet unknown.



292 **Figure 1** Swept chromosomes and genetic relatedness of wild *C. elegans* isotypes. (A)  
293 Sharing of the most common haplotypes (red) across the genome of *C. elegans* for 403  
294 isotypes is shown. Genomic regions of unswept haplotypes (haplotypes other than the  
295 most common haplotypes) are colored gray. White segments are undetermined  
296 haplotypes in regions where no identical-by-descent groups were found (Crombie *et al.*  
297 2019). The genomic position is plotted on the x-axis. Each row on the y-axis represents  
298 one of the 403 isotypes, ordered as their positions in (B). (B) A tree showing genetic  
299 relatedness of the 403 *C. elegans* isotypes, using 1,074,596 biallelic segregating sites, is  
300 shown. The tips of the tree are colored by the number of swept chromosomes (purple for  
301 zero, deep blue for one, light blue for two, orange for three, and gold for four) in each *C.  
302 elegans* isotype.  
303

304 **Natural variation in fertility among swept and divergent strains**

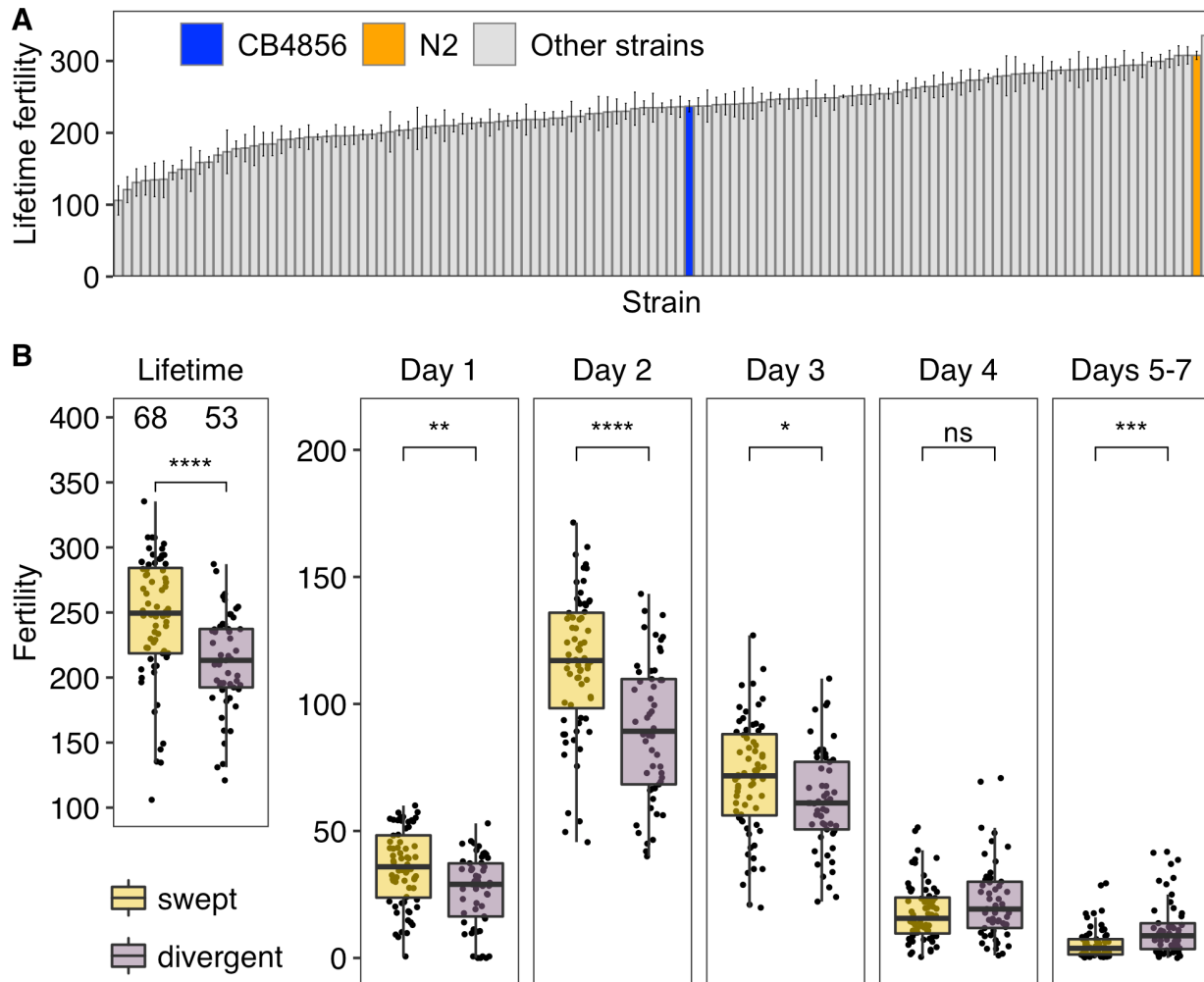
305 To compare the fitness between swept and divergent isotypes, we measured lifetime  
306 fertility of 121 wild *C. elegans* strains sampled across the globe (Figure S1, File S8).  
307 Single fourth larval stage hermaphrodites were transferred daily for five days and  
308 maintained under normal laboratory conditions. We manually counted the viable offspring  
309 from images of assay plates. The results showed large variation in lifetime fertility among  
310 wild *C. elegans* strains (Figure 2A, File S3). The mean lifetime fertility ranged from 106 to  
311 335 offspring among the 121 strains. We observed the species reproductive peak in the  
312 second day of the assay, with a median peak number of 109 offspring (Figure 2B, File  
313 S4).

314 Of the 121 *C. elegans* strains, 68 strains were classified as “swept” strains and 53  
315 strains were classified as “divergent” strains (see Methods, Figure 2B, Figure S1, File  
316 S3). Mean lifetime fertility of swept strains was significantly higher than divergent strains  
317 (Wilcoxon test,  $p = 9.1\text{E-}6$ ) (Figure 2B). Because different strains could have different  
318 swept chromosomes, we extended the comparisons to chromosome levels (Figure S2,  
319 File S9). We assigned strains into swept groups or divergent groups in each swept  
320 chromosome, depending on whether isotypes had a specific swept chromosome.

321 Although the numbers of strains in the two groups were different across swept  
322 chromosomes, swept groups always showed significantly higher lifetime fertility than  
323 divergent groups (Wilcoxon test,  $p < 0.0001$ ) (Figure S2). The striking differences in  
324 lifetime fertility suggested that swept strains have higher fitness than divergent strains  
325 under normal laboratory conditions. Additionally, we compared the daily fertility between  
326 swept and divergent strains. We found that swept strains showed significantly higher daily  
327 fertility than divergent strains in the first three days of the assays (Wilcoxon test,  $p =$   
328 0.0016,  $p = 1.7\text{E-}6$ , and  $p = 0.014$ , respectively) (Figure 2B). This significant difference of  
329 fertility between swept and non-swept groups provided an opportunity to dissect the  
330 genetic basis of the natural variation in lifetime fertility. We calculated the broad-sense  
331 heritability and found a substantial heritable genetic component ( $H^2 = 0.63$ ) of the  
332 phenotypic variance across these strains.

333

334



335

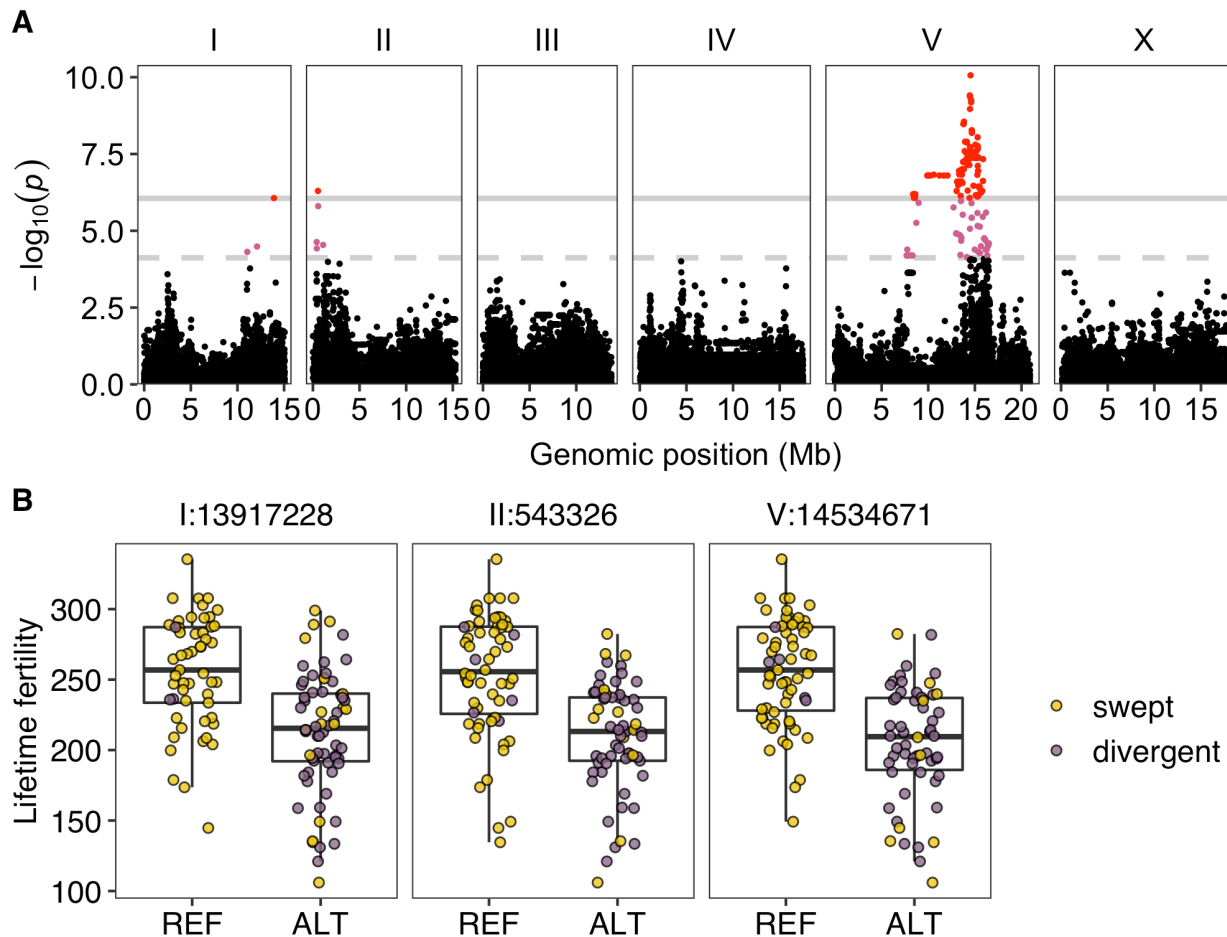
336 **Figure 2** Natural variation in *C. elegans* fertility. (A) A bar plot for lifetime fertility (y-axis)  
337 of 121 wild *C. elegans* strains is shown. Strains on the x-axis are sorted by their mean  
338 lifetime fertility of two to five biological replicates. Error bars show standard errors of  
339 lifetime fertility among replicates. The lab reference strain N2 and the Hawaii strain  
340 CB4856 are colored orange and blue, respectively; other strains are colored gray. (B)  
341 Comparisons of lifetime and daily fertility between 68 swept strains (gold) and 53  
342 divergent strains (purple) are shown as Tukey box plots. Statistical significance was  
343 calculated using the Wilcoxon test. Significance of each comparison is shown above each  
344 comparison pair (ns: p-value > 0.05; \*: p-value ≤ 0.05; \*\*: p-value ≤ 0.01; \*\*\*: p-value ≤  
345 0.001; \*\*\*\*: p-value ≤ 0.0001).

346

347 **Three QTL are associated with natural variation in *C. elegans* lifetime fertility**

348 To identify genomic loci that underlie fertility variation, we performed a marker-based  
349 GWA mapping using mean lifetime fertility data from 121 *C. elegans* strains and the

350 whole-genome variant data from CeNDR. We identified three distinct QTL (Figure 3A,  
351 File S5). The first QTL, located on the right arm of chromosome I, has a peak-marker at  
352 position 13,917,228 and explains 21% of the phenotypic variation among the 121 strains.  
353 The second QTL located on the left arm of chromosome II has a peak-marker position at  
354 543,326 and explains 22% of the phenotypic variation. The third QTL spans the center of  
355 chromosome V with the peak marker located at 14,534,671 and explains 30% of the  
356 phenotypic variation. Because of the strong LD within and between chromosomes in *C.*  
357 *elegans* (Andersen *et al.* 2012), linked regions might be falsely discovered as QTL even  
358 though they have no variants that underlie the phenotypic variation. To test the  
359 independence of the three QTL, we calculated the pairwise LD among their peak markers  
360 (Figure S3, File S10). The results showed moderate levels of LD (ranged from 0.387 to  
361 0.512) for all three pairs, suggesting that they might not be independent. Notably, at all  
362 QTL peak markers, most swept strains have the reference alleles and most divergent  
363 strains have the alternative alleles (Figure 3B, File S6). We further compared the sharing  
364 of haplotypes among the 121 strains within each QTL region (Figure S4, File S11). The  
365 majority of the strains with the reference alleles at the peak markers have the most  
366 common haplotypes in the QTL regions. By contrast, few strains with alternative alleles  
367 have the most common haplotypes in the QTL regions. Taken together, these results  
368 suggest that the genetic variants and different haplotypes underlying lifetime fertility  
369 variation might be linked to the selective sweeps in the global population of *C. elegans*.



370

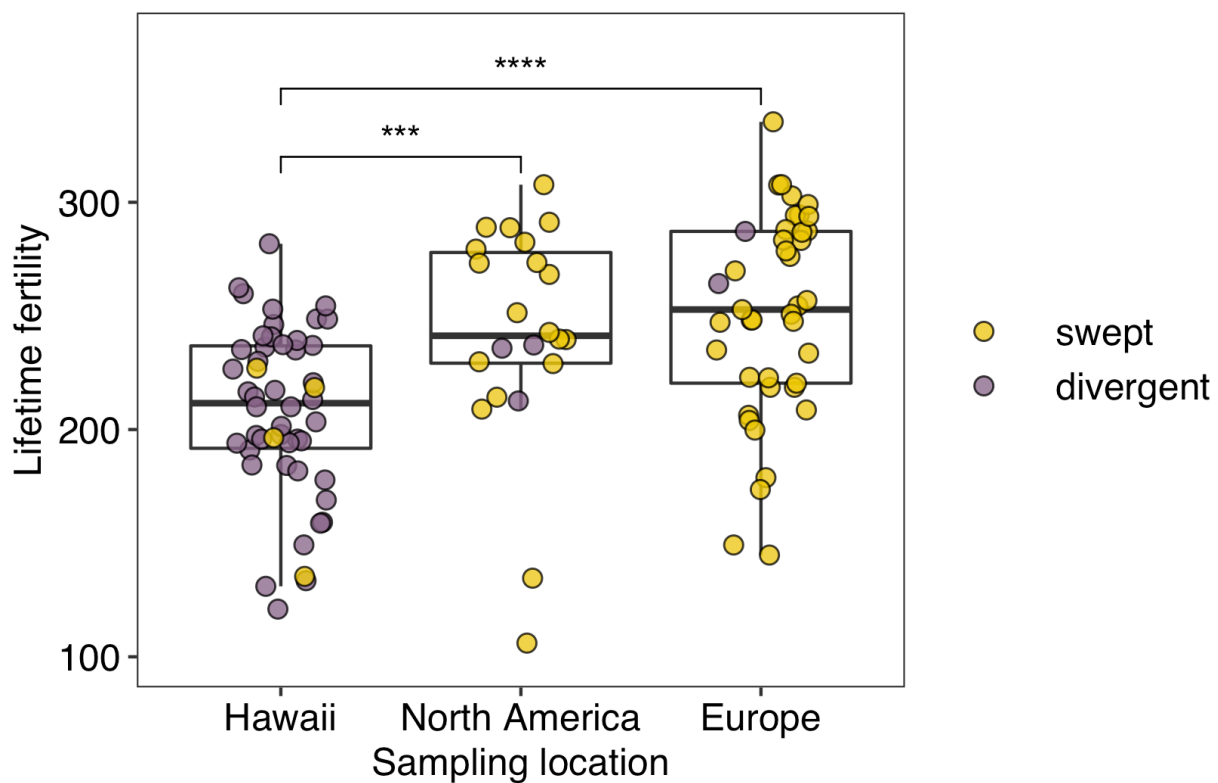
371 **Figure 3** Three QTL were identified in GWA mapping of lifetime fertility variation in 121  
372 *C. elegans* wild strains. (A) Manhattan plot indicating GWA mapping results. Each point  
373 represents an SNV that is plotted with its genomic position (x-axis) against its  $-\log_{10}(p)$   
374 value (y-axis) in mapping. SNVs that pass the genome-wide EIGEN threshold (the dotted  
375 gray horizontal line) and the genome-wide BF threshold (the solid gray horizontal line)  
376 are colored pink and red, respectively. (B) Tukey box plots showing lifetime fertility  
377 between strains with different genotypes at the peak marker position in each QTL. Each  
378 point corresponds to a *C. elegans* strain and is colored gold for swept strains and purple  
379 for divergent strains. On the x-axis, REF represents strains with the N2 reference allele  
380 and ALT represents strains with the alternative allele.  
381

382 **Hawaiian *C. elegans* exhibit lower lifetime fertility than strains sampled across the**  
383 **globe**

384 Most of the 121 *C. elegans* strains were originally sampled from three geographically  
385 isolated locations: 50 from the Hawaiian Islands, 22 from North America, and 41 from

386 Europe (Figure S1). Of the 50 Hawaiian *C. elegans* strains, 46 were classified as  
387 divergent, and the other four strains have no more than two swept chromosomes (Figure  
388 4, Figure S1, File S7). Most *C. elegans* strains from North America and Europe were  
389 classified as swept strains (Figure 4, Figure S1, File S7). We compared lifetime fertilities  
390 of strains isolated from these three locations (Figure 4). Compared to strains from North  
391 America and Europe, Hawaiian strains had significantly lower lifetime fertility (Wilcoxon  
392 test,  $p = 0.00063$  and  $p = 7.5\text{E-}6$ , respectively). The difference in lifetime fertility between  
393 strains from North America and strains from Europe was insignificant. These data  
394 suggested that the selective sweeps that occurred outside Hawaii contribute substantially  
395 to the geographical lifetime fertility difference.

396



397

398 **Figure 4** Lifetime fertility comparisons in wild *C. elegans* strains among different sampling  
399 locations. Comparisons of lifetime fertility among strains collected from Hawaii (50

400 strains), North America (22 strains), and Europe (41 strains). Each point corresponds to  
401 a strain and is colored gold for swept strains and purple for divergent strains. Statistical  
402 significance was calculated using the Wilcoxon test. Significance of each comparison is  
403 shown above each comparison pair (\*\*: p-value ≤ 0.001; \*\*\*\*: p-value ≤ 0.0001). The  
404 difference of lifetime fertility between North American and European strains is  
405 insignificant.

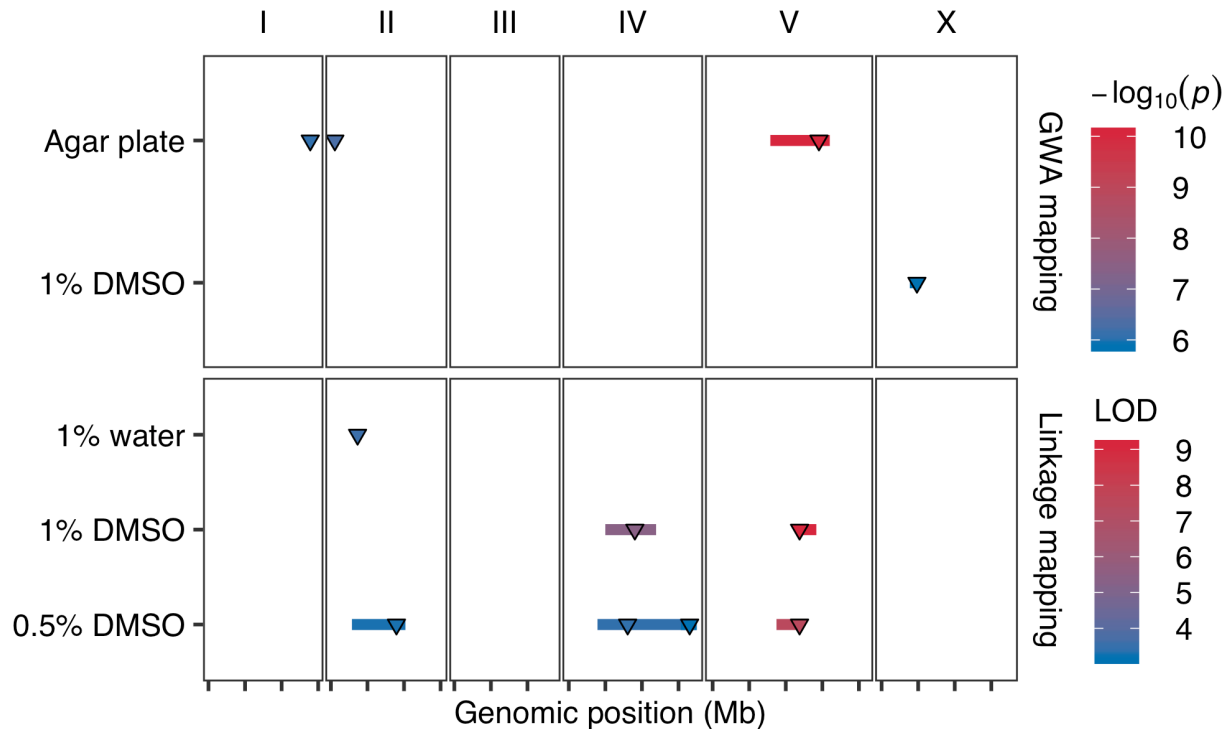
406

407 **More QTL underlying lifetime fertility of *C. elegans***

408 We also mapped the fertility data in the 1% DMSO control condition from one of our  
409 published studies that used the high-throughput fitness assays (HTA) (See Methods) to  
410 measure various fitness parameters of 236 strains (209 swept strains and 27 divergent  
411 strains) (Hahnel *et al.* 2018). Here, we performed GWA mapping using the fertility  
412 measurements (norm.n) and identified a QTL on chromosome X (from 3.9 Mb to 5.4 Mb,  
413 with the peak marker at 4,831,537) (Figure 5, Figure S5A, File S12). Divergent strains  
414 showed no enrichment with either genotype at the peak marker (Figure S5B, File S13).  
415 However, most strains with the reference allele have the most common haplotypes and  
416 most strains with the alternative allele have unswept haplotypes (Figure S5C, File S14).  
417 These results suggest that the genetic variants in this region might also be linked to the  
418 recent selective sweeps in wild *C. elegans* populations.

419 Also using HTA as above, we measured fertility in liquid culture using the *C.*  
420 *elegans* recombinant inbred advanced intercross lines (RIAILs) derived from QX1430 and  
421 CB4856 (Andersen *et al.* 2015) under three conditions: 1% water, 1% DMSO, and 0.5%  
422 DMSO (see Methods). In contrast to the fertility variation of *C. elegans* strains cultured in  
423 agar plates, the N2 strain showed lower fertility than the CB4856 strain using HTA (Figure  
424 S6B, Figure S7B, Figure S8B, File S16, File S18, File S20), indicating that environmental  
425 factors can have drastic effects on *C. elegans* fertility. We found seven QTL for fertility on

426 chromosomes II, IV, and V under the three conditions (Figure 5, Figure S6A, Figure S7A,  
427 Figure S8A). In 1% water, linkage mapping identified a single QTL confidence interval (II:  
428 3.4 Mb - 4 Mb) on the left arm of chromosome II (Figure 5, Figure S6A, File S15). In 1%  
429 DMSO, linkage mapping identified two QTL located on chromosomes IV (5 Mb - 11.9 Mb)  
430 and V (11.8 Mb - 14.2 Mb), respectively (Figure 5, Figure S7A, File S17). In 0.5% DMSO,  
431 the four QTL on chromosomes II (2.9 Mb - 10.2 Mb), IV (3.9 Mb - 17.5 Mb), and V (8.7  
432 Mb - 12.3 Mb) recapitulated the three QTL detected in 1% water and 1% DMSO,  
433 respectively (Figure 5, Figure S8A, File S19). Furthermore, the QTL on chromosome V in  
434 both DMSO conditions overlapped with the GWA QTL on chromosome V using the 121  
435 wild strains in agar plates (Figure 5). Because linkage mapping using this set of *C.*  
436 *elegans* RIAILs can only find QTL variants in the CB4856 strain, overlapping of QTL  
437 between linkage mapping and GWA mapping suggests that the CB4856 strain carries the  
438 common alternative alleles among wild *C. elegans* strains in the shared regions.  
439 Altogether, these results suggest that *C. elegans* might have shared and separated loci  
440 controlling fertility in agar cultures and in liquid cultures with slightly different  
441 concentrations of DMSO.



442

443 **Figure 5** Multiple QTL impacting *C. elegans* lifetime fertility in different conditions. Four  
444 GWA mapping QTL of two conditions (121 strains cultured in agar plate and 236 strains  
445 cultured in liquid with 1% DMSO) and seven linkage mapping QTL of three conditions (*C.*  
446 *elegans* RIAILs cultured in liquid with 1% water, 1% DMSO, and 0.5% DMSO,  
447 respectively) are plotted. Each condition is plotted on the y-axis against the genomic  
448 position of its QTL on the x-axis separated by chromosomes with tick marks denoting  
449 every 5 Mb. Each QTL is plotted as a line with a triangle indicating the peak marker and  
450 colored by the  $-\log_{10}(p)$  value (GWA QTL) or the logarithm of the odds (LOD) score (for  
451 linkage mapping QTL), increasing in significance from blue to red.  
452

453

## DISCUSSION

454 In this study, we report natural variation of lifetime fertility for 121 wild *C. elegans* strains  
455 and found that the previously reported chromosome-scale selective sweeps play a key  
456 role in the different fertilities among strains. We defined swept haplotypes, swept isotypes,  
457 and swept strains, using the latest *C. elegans* haplotype data from CeNDR. Swept strains  
458 that have at least one chromosome with equal or greater than 30% of swept haplotypes  
459 showed significantly higher lifetime fertility than divergent strains that have avoided the  
460 sweeps. We identified three QTL that underlie differences in lifetime fertility among the

461 121 *C. elegans* strains using single-marker based GWA mappings. Remarkably, across  
462 all three QTL, swept strains tend to have shared haplotypes and the reference alleles at  
463 peak markers. By contrast, divergent strains tend to have unswept haplotypes and the  
464 alternative alleles at peak markers. We also observed significant geographical differences  
465 in lifetime fertility between Hawaiian strains and strains from other parts of the world, likely  
466 because of the selective sweeps. We further mapped previous data using GWA mapping  
467 and linkage mapping and identified eight QTL underlying *C. elegans* fertility in different  
468 environments. Taken together, our results showed the diverse genetic basis of *C. elegans*  
469 fertility and suggest that higher fertility in most *C. elegans* strains could be caused by  
470 alleles that have recently swept throughout the world population.

471

472 **Genetically divergent strains have substantially lower fertility than swept strains**

473 We measured lifetime fertility in 121 genetically distinct *C. elegans* strains. In our  
474 measurements (Figure 2A), the laboratory reference strain N2 (known as the Bristol  
475 strain) and a frequently used wild strain CB4856 (known as the Hawaii strain) had lifetime  
476 fertility of 308 and 237, respectively, with similar fertility values as reported previously  
477 (Hodgkin and Doniach 1997; Wegewitz *et al.* 2008; Andersen *et al.* 2014). The CB4856  
478 strain had been considered the most genetically distant strain from the N2 strain for  
479 decades. In the last five years, researchers have collected and identified many genetically  
480 divergent *C. elegans* strains, some of which are more divergent from the N2 strain than  
481 the CB4856 strain is (Cook *et al.* 2017; Crombie *et al.* 2019; Lee *et al.* 2020). Most of  
482 these divergent strains were from Hawaii and showed none or rare evidence of the  
483 globally distributed swept haplotypes (Figure 1, Figure S1) (Crombie *et al.* 2019; Lee et

484 *al.* 2020). In our fertility assays, we included many of these divergent strains. Under  
485 normal laboratory conditions, divergent strains showed significantly lower fertility than  
486 swept strains that have large blocks of swept haplotypes, suggesting that divergent  
487 strains have lower fitness than swept strains. The disadvantage in fertility of divergent  
488 strains was present from the beginning of the reproductive period throughout the peak.  
489 This lower fitness of divergent strains could have at least two possible explanations. First,  
490 laboratory conditions might favor swept strains over divergent strains. Standard  
491 laboratory conditions to culture *C. elegans* have been designed, modified, and improved  
492 based on the growth of the N2 strain (Brenner 1974), which is a swept strain. Most swept  
493 strains were from temperate zones (Andersen *et al.* 2012; Félix and Duveau 2012;  
494 Petersen *et al.* 2014; Richaud *et al.* 2018), such as Western Europe, whereas most  
495 divergent strains were isolated in the high elevation and cool temperature niches in the  
496 Hawaiian Islands (Crombie *et al.* 2019). The conditions of the natural habitats and the  
497 microenvironments in the niches of swept strains could be drastically different from niches  
498 of divergent strains. The closer the natural niche condition is to the laboratory condition,  
499 the higher fitness a swept strain might have. For instance, compared to N2, the strain  
500 CB4856 showed a clear thermal preference of approximately 17°C, which is lower than  
501 the canonical and the most typical *C. elegans* culture temperature of 20°C in the  
502 laboratory (Brenner 1974; Stiernagle 2006; Anderson *et al.* 2007). In a competition assay  
503 between two swept strains that isolated from locations with distinct climates, CX11314  
504 (isolated at 20.9 °C) showed higher fitness than JU847 (isolated at 11.3°C) at both 15°C  
505 and 25°C, but JU847 grew better at 15°C than at 25°C (Evans *et al.* 2017). Divergent  
506 strains that were isolated from cool regions might exhibit higher fitness at temperatures

507 lower than 20°C. The second explanation is that genetic variants at unknown loci directly  
508 caused differences in lifetime fertility between swept strains and divergent strains. The  
509 environment factors in our assays might have similar or minor influences on the fertility  
510 for both swept strains and divergent strains. The major differences in fertility between  
511 swept strains and divergent strains could be attributed to their genetic differences. For  
512 instance, because a *C. elegans* hermaphrodite produces 200 - 300 sperm in the late L4  
513 stage before irreversibly switching to oogenesis to produce up to 1000 oocytes, the  
514 number of sperm limits fertility of self-fertilized hermaphrodites (Ward and Carrel 1979;  
515 Cutter 2004; Félix and Braendle 2010). Alleles at unknown loci in swept strains might lead  
516 to an increased number of sperm and thus a higher fertility than divergent strains. It is  
517 also possible that swept strains and divergent strains produce similar numbers of sperm,  
518 but divergent strains have higher embryonic lethality than swept strains. Because we  
519 quantified the viable offspring of each *C. elegans* strains as their fertility (See Methods),  
520 higher embryonic lethality could have caused the lower fertility in divergent strains.  
521 Although our GWA results might have mapped genomic regions underlying  
522 spermatogenesis or embryonic lethality, future efforts to quantify the numbers of sperm  
523 and fertilized embryos among wild *C. elegans* strains will help to further elucidate the  
524 differences in fertility among strains.

525

## 526 **Diverse QTL for lifetime fertility in different environments**

527 We performed GWA mapping and identified three QTL on chromosome I, II, and V for  
528 lifetime fertility of *C. elegans*, which were grown on agar plates and fed *E. coli* OP50. The  
529 split of strains by genotypes at peak markers and the haplotypes of each strain in each

530 QTL strongly suggest that the three QTL could be the genetic basis of different lifetime  
531 fertility between swept strains and divergent strains. The reference alleles and the most  
532 common haplotypes in each QTL, which provided the selective advantage of higher  
533 fertility, could have swept through the *C. elegans* population as these strains spread  
534 throughout the world. Under similar conditions, a previous study using linkage mapping  
535 and a large panel of RIAILs derived from the N2 and CB4856 strains have mapped fertility  
536 to QTL on chromosome II (2.6 Mb - 3.6 Mb) and X (4.6 Mb - 7.7 Mb) (Andersen *et al.*  
537 2014). A laboratory-derived mutation in the gene *npr-1* from N2 was identified to have  
538 driven the QTL on chromosome X (McGrath *et al.* 2009; Andersen *et al.* 2014).

539 In liquid culture and fed the *E. coli* strain HB101, a new panel of *C. elegans* RIAILs  
540 with replacement of the N2 *npr-1* allele with the counterpart version from the CB4856  
541 strain was used to map fertility to a QTL on chromosome IV (10.7 Mb - 12.8 Mb) by linkage  
542 mapping (Andersen *et al.* 2015). Using the same RIAILs panel but under three different  
543 liquid conditions (1% H<sub>2</sub>O, 1% DMSO, and 0.5% DMSO), we mapped fertility to seven  
544 QTL on chromosome II, IV, and V. In both DMSO conditions, the three QTL on  
545 chromosome IV recapitulated the QTL in the above study (Andersen *et al.* 2015); the two  
546 overlapping QTL on chromosome V overlapped with the QTL using our 121 wild strains  
547 grown in agar plates. We further used GWA to map previously published wild strain fertility  
548 data from liquid culture and 1% DMSO. A QTL linked to the selective sweeps located on  
549 the left arm of chromosome X was identified. Although *npr-1* is in the region of this QTL,  
550 the laboratory-derived N2 *npr-1* allele that is only found in the N2 strain could not drive  
551 this QTL because it is not found in wild strains.

552 As a complex life history trait, lifetime fertility could be influenced by many loci  
553 (Houle 1992). Under different conditions, GWA mappings identified QTL on chromosome  
554 I, II, V, and X; linkage mappings identified QTL on chromosome II, IV, V, and X. These  
555 results suggest that shared and separate loci in *C. elegans* genome control fertility in  
556 various environmental conditions. Because swept haplotypes shared among *C. elegans*  
557 strains might have driven all the QTL in GWA mappings, genetic variants in these swept  
558 haplotypes might be the beneficial alleles that swept through the *C. elegans* population.

559

560 **Potential adaptive alleles for *C. elegans* in temperate zones**

561 The QTL for lifetime fertility using the 121 *C. elegans* strains also shared genomic regions  
562 with QTL on weather and climate variables related to natural habitats of 149 wild *C.*  
563 *elegans* strains (Evans *et al.* 2017). Two of the GWA mapping QTL for relative humidity  
564 were on chromosomes II and V, which overlapped with our QTL on chromosomes II and  
565 V, respectively. GWA mappings for three-year average temperature also located the  
566 same QTL just right of the center of chromosome V. We showed that *C. elegans* strains  
567 sampled from Europe and North America had similar lifetime fertilities, which were  
568 significantly larger than fertilities of Hawaiian *C. elegans* strains. Because Hawaii is in the  
569 tropical zone, *C. elegans* isolated from high elevation areas in Hawaii could have  
570 experienced high humidity and low temperatures in a much more stable climate in the  
571 long term than *C. elegans* in temperate zones. Alleles of swept strains in the shared QTL  
572 underlying lifetime fertility and climate variables could have enhanced the adaptability of  
573 *C. elegans* to variable humidity and temperatures in temperate zones along the *C.*  
574 *elegans* expansion out of the Pacific region (Andersen *et al.* 2012; Crombie *et al.* 2019;

575 Lee *et al.* 2020). It is possible that, because of these adaptive alleles, the N2 strain  
576 showed no preference at these temperatures (Anderson *et al.* 2007).

577 Some Hawaiian strains, exclusively isolated at lower elevations closer to the  
578 coasts, exhibited admixture with non-Hawaiian populations, which might come from gene  
579 flow from outcrossing with immigrating swept strains from outside to Hawaii (Crombie *et*  
580 *al.* 2019). But compared to most non-Hawaiian strains, Hawaiian strains only contain, if  
581 any, small fractions of swept haplotypes. Of the 50 Hawaiian *C. elegans* strains used in  
582 this study, four strains are classified as swept strains, who have no more than two swept  
583 chromosomes (Figure S1). The alleles that increase lifetime fertility in swept strains might  
584 not contribute to higher fitness for *C. elegans* strains in Hawaii. In fluctuating  
585 environments in temperate zones, the randomly distributed and limited habitats might  
586 select for *C. elegans* that have higher fertility, although the high density of animals also  
587 facilitates dauer formation, which could underlie future survival success. Moreover, *C.*  
588 *elegans* populations in temperate zones also undergo bottlenecks in winter, from which  
589 dauers are more likely to survive. By contrast, Hawaiian *C. elegans* might not need to  
590 enter and stay in the dauer stage as often and long as non-Hawaiian *C. elegans* in  
591 temperate zones. Ample available habitats (e.g. rotting fruits) and the stable environment  
592 in Hawaii could lead to a higher survival rate for *C. elegans*, and thus lower fertility as a  
593 trade-off.

594

595

596

597

598 **ACKNOWLEDGMENTS**

599 We would like to thank members of the Andersen Lab for helpful comments on the  
600 manuscript. G.Z. received support from the NSF-Simons Center for Quantitative Biology  
601 at Northwestern University (awards Simons Foundation/SFARI 597491-RWC and the  
602 National Science Foundation 1764421). J.D.M received support from a Northwestern  
603 Undergraduate Research Grant.

604

605

606

607

608

609

610

611

612

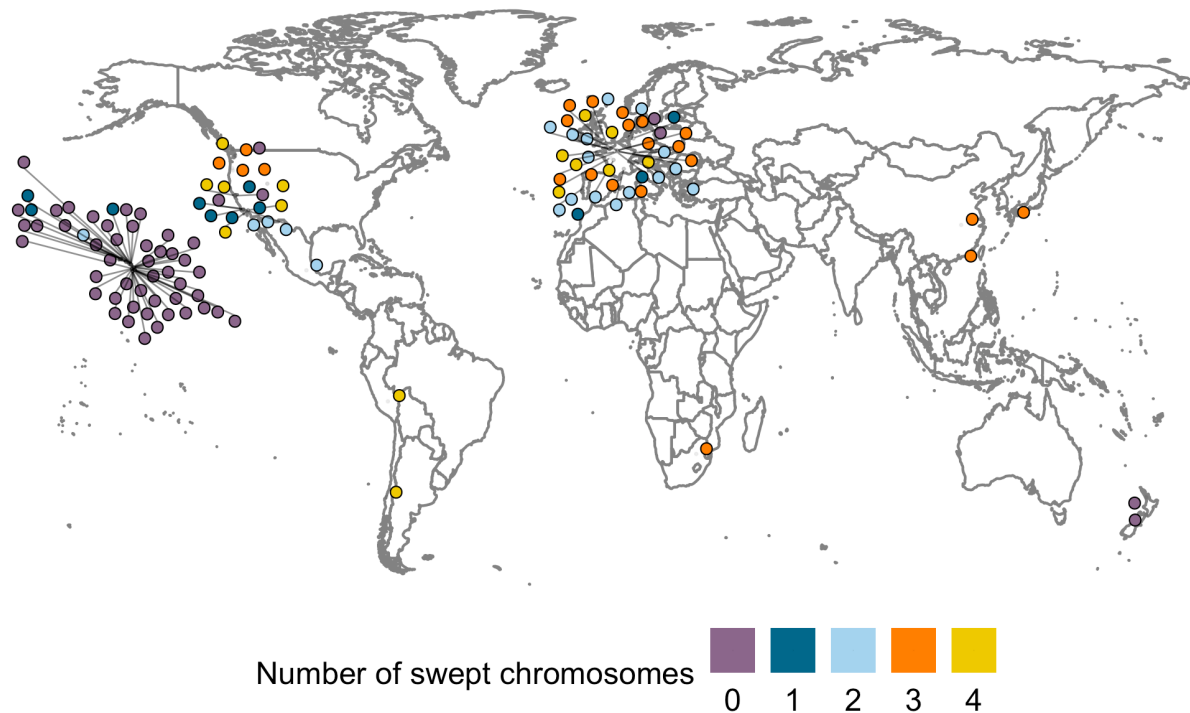
613

614

615

616

617

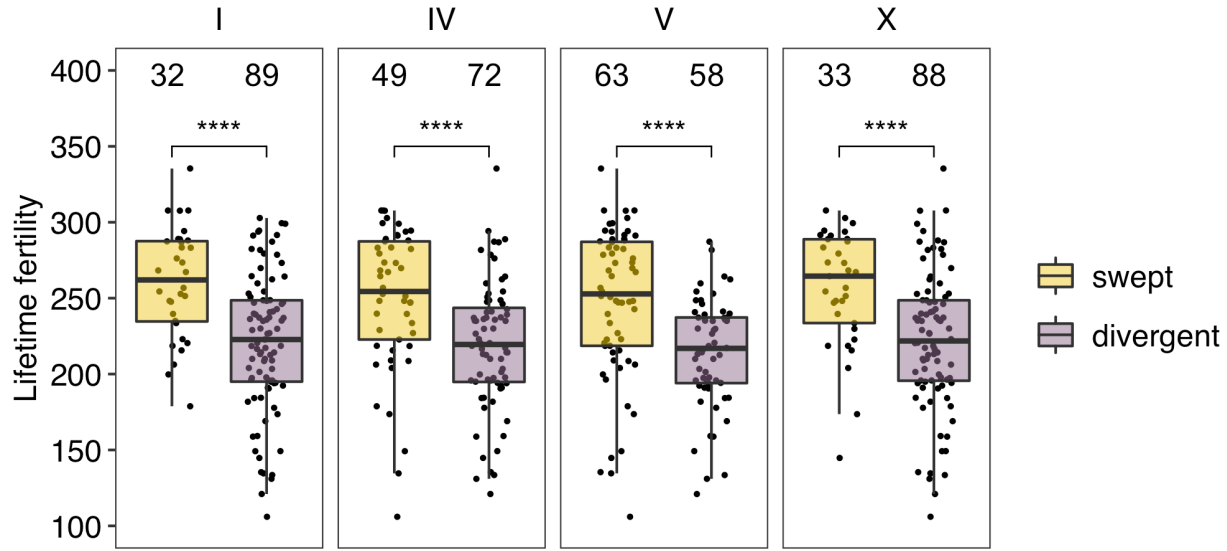


618

619 **Figure S1** Global distribution of the 121 wild *C. elegans* strains used in this study. Each  
620 point corresponds to the isolation location and is colored by the number of swept  
621 chromosomes.

622

623



624

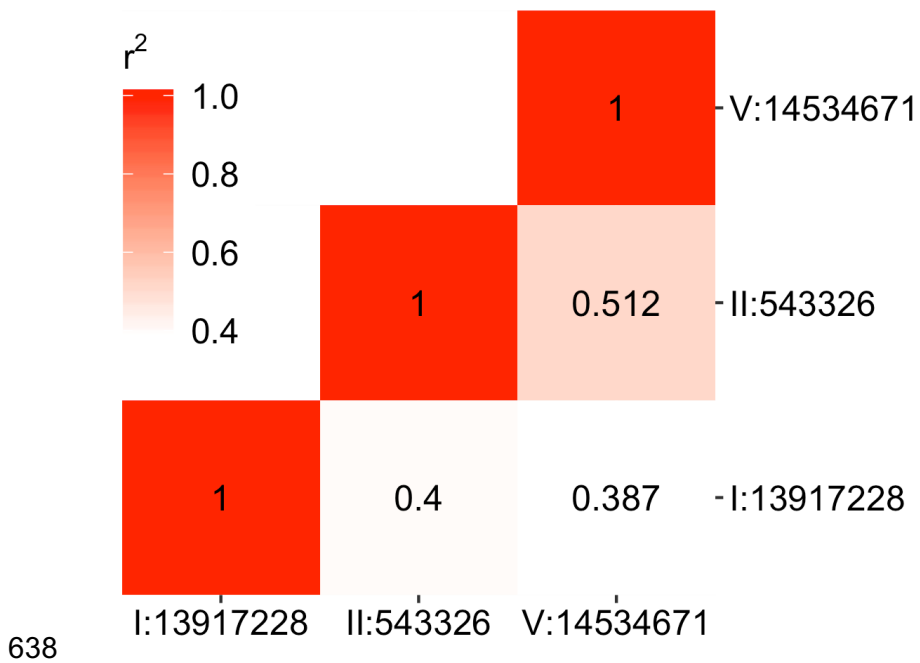
625 **Figure S2** Comparisons of *C. elegans* lifetime fertility between swept groups (gold) and  
626 divergent groups (purple) classified by single chromosome are shown as Tukey box plots.  
627 Only swept chromosomes (I, IV, V, and X) are shown. For each chromosome (panel),  
628 strains with swept chromosomes were assigned to swept groups; strains with divergent  
629 chromosomes were assigned to divergent groups. Statistical significance was calculated  
630 using the Wilcoxon test, with  $p$ -values 3.7E-5, 5.5E-5, 6.5E-6, and 6.6E-5 in the  
631 comparisons by chromosomes I, IV, V, and X, respectively. Significance of each  
632 comparison is shown above each comparison pair (\*\*\*\*:  $p$ -value  $\leq 0.0001$ ). The number  
633 of strains in each group is indicated above significance.

634

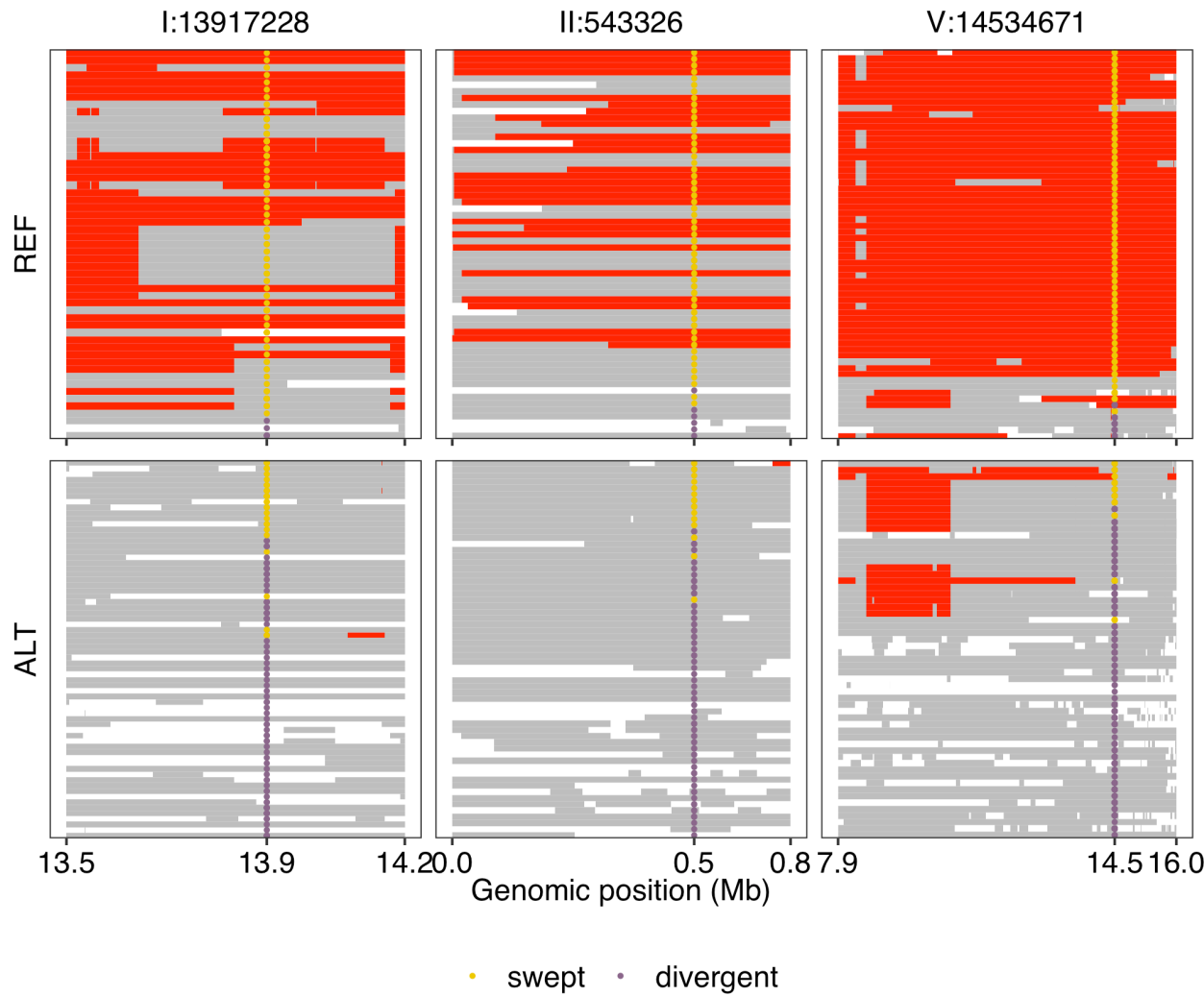
635

636

637

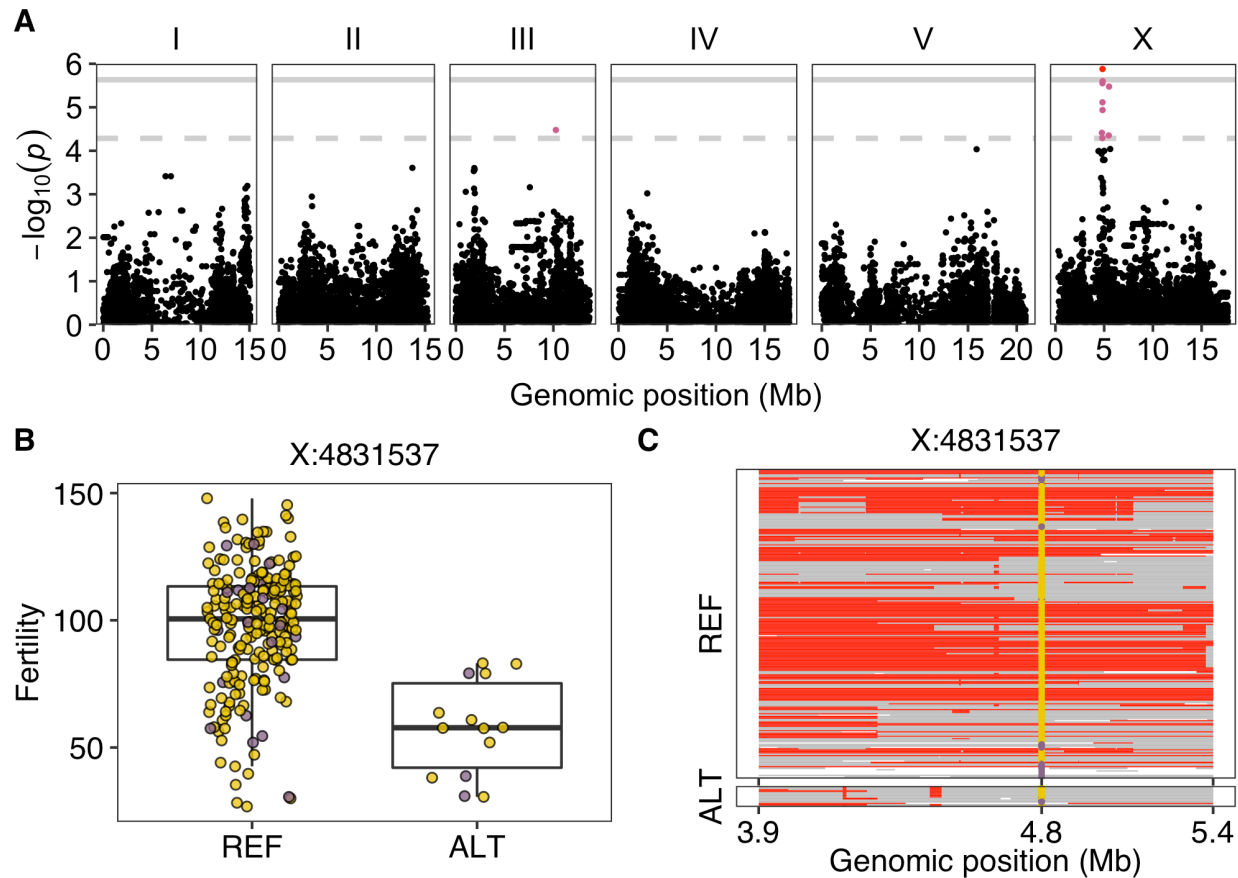


638  
639 **Figure S3** Linkage disequilibrium of QTL peak markers associated with *C. elegans*  
640 lifetime fertility is shown. Correlations ( $r^2$ ) between each marker pair are indicated in the  
641 tiles and are represented by the tile color.



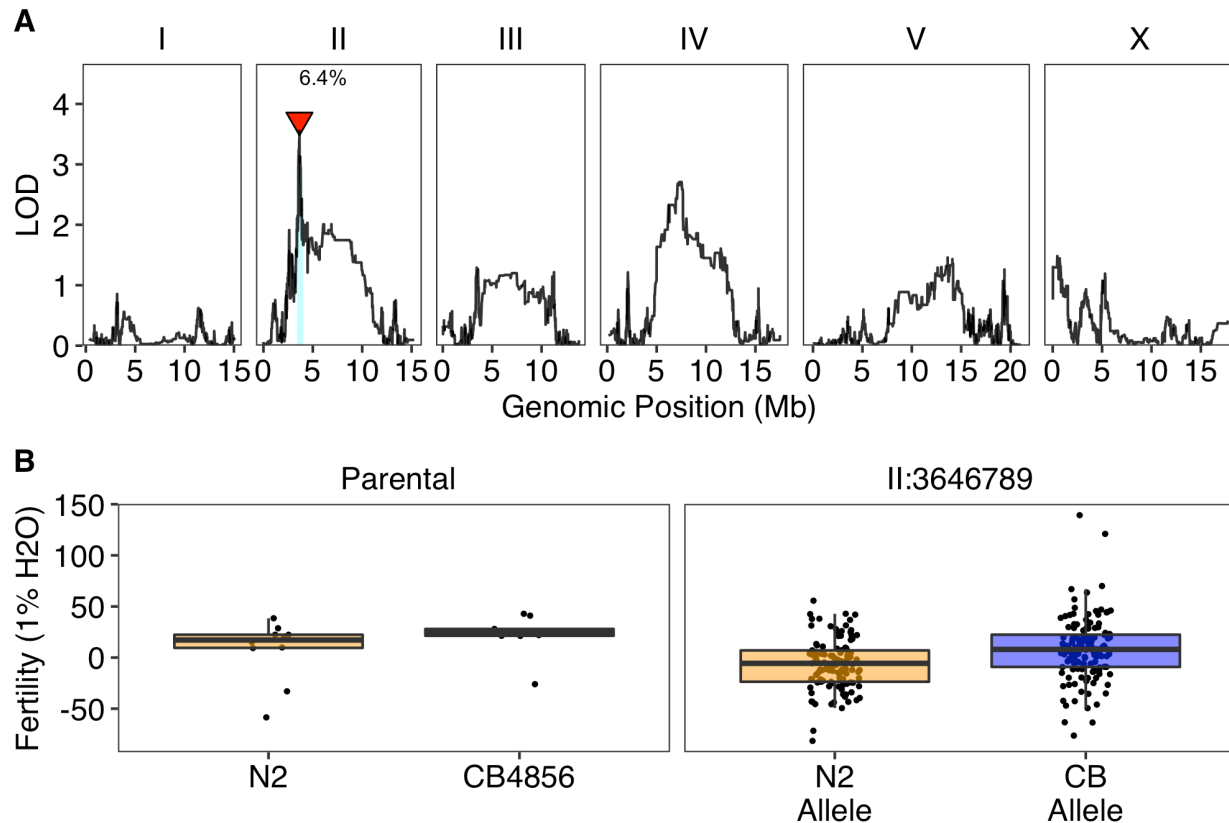
642

643 **Figure S4** Sharing of haplotypes within QTL associated with lifetime fertility variation  
644 among 121 *C. elegans* strains is shown. Genomic regions of most common, rare and  
645 undetermined haplotypes are colored red, gray, and white, respectively. For each QTL  
646 (represented by peak markers on the top), strains were divided into REF (N2 reference  
647 alleles) panels or ALT (alternative alleles) panels by their genotypes at the peak markers  
648 as in Figure 3B. The genomic positions of each QTL are plotted on the x-axis. In the two  
649 panels of each QTL, each row on the y-axis represents one of the 121 strains and is  
650 ordered by their relative positions in Figure 1B. Swept strains and divergent strains are  
651 indicated as gold dots and purple dots, respectively, at the peak markers.



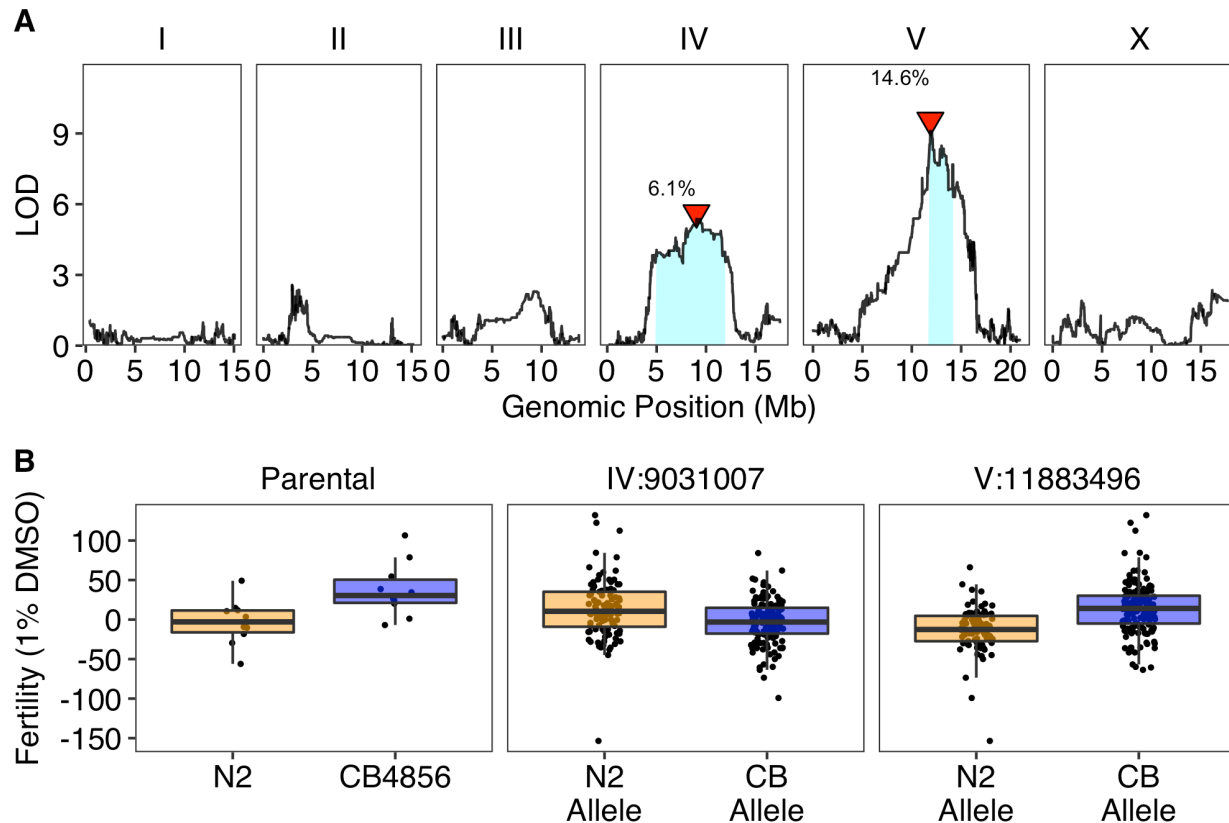
652

653 **Figure S5** One QTL was identified in GWA mapping of *C. elegans* fertility variation in 236  
654 strains. (A) Manhattan plot indicating GWA mapping results. Each point represents an  
655 SNV that is plotted with its genomic position (x-axis) against its  $-\log_{10}(p)$  value (y-axis) in  
656 mapping. SNVs that pass the genome-wide EIGEN threshold (the dotted gray horizontal  
657 line) and the genome-wide BF threshold (the solid gray horizontal line) are colored pink  
658 and red, respectively. (B) Tukey box plot showing fertility (norm.n) between strains with  
659 different genotypes at the peak marker position in the QTL. Each point corresponds to a  
660 *C. elegans* strain and is colored gold for swept strains and purple for divergent strains.  
661 On the x-axis, REF represents strains with the N2 reference allele and ALT represents  
662 strains with the alternative allele. (C) Sharing of haplotypes within the QTL is shown.  
663 Genomic regions of most common, rare and undetermined haplotypes are colored red,  
664 gray, and white, respectively. Strains were divided into REF (N2 reference alleles) panels  
665 or ALT (alternative alleles) panels by their genotypes at the peak markers as in (B). The  
666 genomic positions of the QTL are plotted on the x-axis. In the two panels of the QTL, each  
667 row on the y-axis represents one of the 236 strains, ordered as their relative positions in  
668 Figure 1B. Swept strains and divergent strains are indicated as gold dots and purple dots,  
669 respectively, at the peak markers.



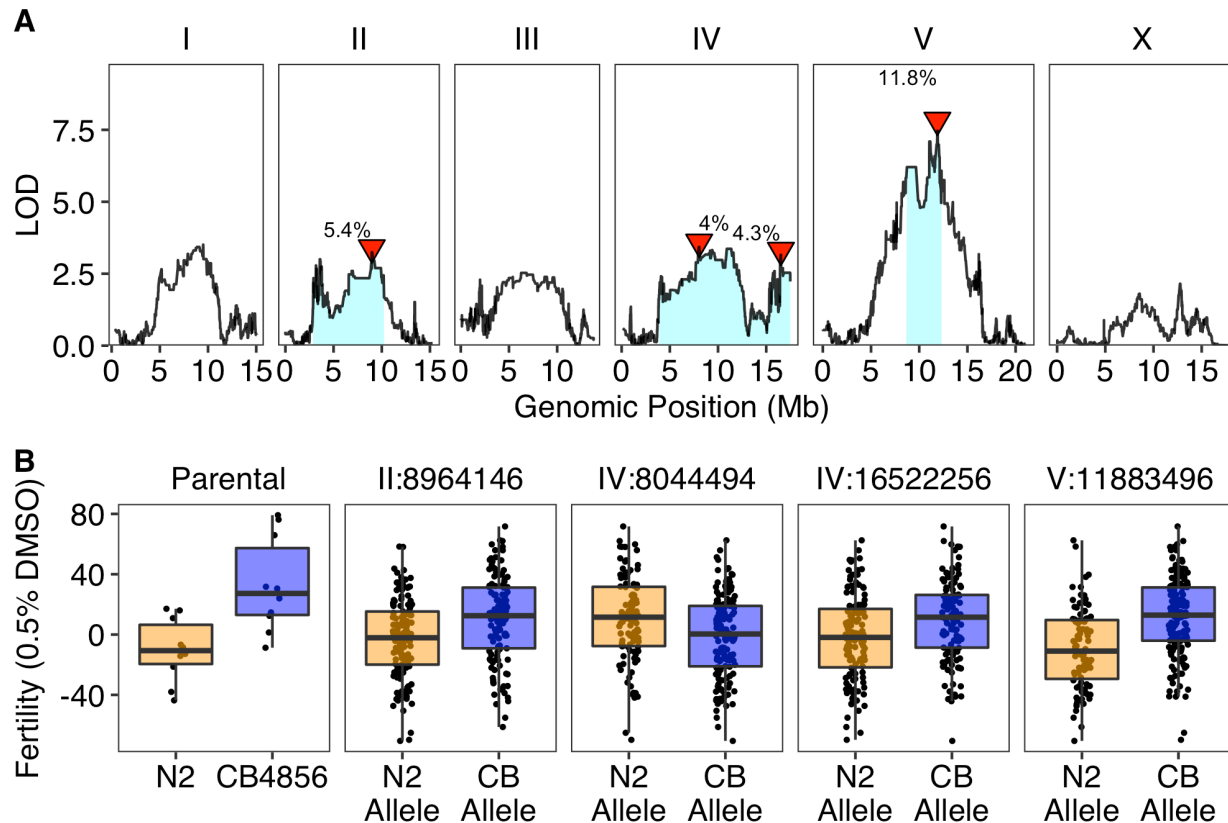
670

671 **Figure S6** A QTL was identified using linkage mapping of *C. elegans* fertility (norm.n) in  
672 1% water conditions. (A) Linkage mapping results of *C. elegans* fertility (norm.n) with  
673 RILs were shown with genomic position in Mb (x-axis) plotted against the logarithm of  
674 the odds (LOD) score (y-axis). The peak marker of the QTL on the left arm of chromosome  
675 II is indicated by a red triangle, next to which the percentage of the total phenotypic  
676 variance that can be explained by the QTL is shown. The 95% confidence interval of the  
677 QTL is shown by a blue rectangle. (B) Fertility (norm.n) is shown between the parents  
678 (N2 and CB4856) and between RILs split by genotype at the peak marker of the QTL.  
679 Each dot in the parental panel represents one of the replicates. Each dot in the QTL panel  
680 corresponds to a unique recombinant strain. Strains with the N2 allele are colored orange,  
681 and strains with the CB4856 allele are colored blue.



682

683 **Figure S7** Two QTL were identified using linkage mapping of *C. elegans* fertility (norm.n)  
684 in 1% DMSO conditions. (A) Linkage mapping results of *C. elegans* fertility (norm.n) with  
685 RIAILs were shown with genomic position in Mb (x-axis) plotted against the logarithm of  
686 the odds (LOD) score (y-axis). The peak markers of QTL are indicated by red triangles,  
687 next to which the percentages of the total phenotypic variance that can be explained by  
688 the QTL are shown. The 95% confidence interval of each QTL is shown by a blue  
689 rectangle. (B) Fertility (norm.n) is shown between the parents (N2 and CB4856), and  
690 between RIAILs split by genotype at the peak marker for each QTL. Each dot in the  
691 parental panel represents one of the replicates. Each dot in each of the QTL panels  
692 corresponds to a unique recombinant strain. Strains with the N2 allele are colored orange  
693 and strains with the CB4856 allele are colored blue.



694

695 **Figure S8** Four QTL were identified using linkage mapping of *C. elegans* fertility (norm.n)  
696 in 0.5% DMSO conditions. (A) Linkage mapping results of *C. elegans* fertility (norm.n)  
697 with RIAILs were shown with genomic position in Mb (x-axis) plotted against the logarithm  
698 of the odds (LOD) score (y-axis). The peak markers of QTL are indicated by red triangles,  
699 next to which the percentages of the total phenotypic variance that can be explained by  
700 the QTL are shown. The 95% confidence interval of each QTL is shown by a blue  
701 rectangle. (B) Fertility (norm.n) is shown between the parents (N2 and CB4856), and  
702 between RIAILs split by genotype at the peak marker for each QTL. Each dot in the  
703 parental panel represents one of the replicates. Each dot in each of the QTL panels  
704 corresponds to a unique recombinant strain. Strains with the N2 allele are colored orange,  
705 and strains with the CB4856 allele are colored blue.  
706

707

708

709

710

711

712 LITERATURE CITED

- 713 Andersen, E. C., J. S. Bloom, J. P. Gerke, and L. Kruglyak, 2014 A variant in the  
714 neuropeptide receptor npr-1 is a major determinant of *Caenorhabditis elegans*  
715 growth and physiology. *PLoS Genet.* 10: e1004156.
- 716 Andersen, E. C., J. P. Gerke, J. A. Shapiro, J. R. Crissman, R. Ghosh *et al.*, 2012  
717 Chromosome-scale selective sweeps shape *Caenorhabditis elegans* genomic  
718 diversity. *Nat. Genet.* 44: 285–290.
- 719 Andersen, E. C., T. C. Shimko, J. R. Crissman, R. Ghosh, J. S. Bloom *et al.*, 2015 A  
720 Powerful New Quantitative Genetics Platform, Combining *Caenorhabditis elegans*  
721 High-Throughput Fitness Assays with a Large Collection of Recombinant Strains.  
722 *G3* 5: 911–920.
- 723 Anderson, J. L., L. Albergotti, S. Proulx, C. Peden, R. B. Huey *et al.*, 2007 Thermal  
724 preference of *Caenorhabditis elegans*: a null model and empirical tests. *J. Exp. Biol.*  
725 210: 3107–3116.
- 726 Barrière, A., and M.-A. Félix, 2005 High local genetic diversity and low outcrossing rate  
727 in *Caenorhabditis elegans* natural populations. *Curr. Biol.* 15: 1176–1184.
- 728 Barrière, A., and M.-A. Félix, 2007 Temporal dynamics and linkage disequilibrium in  
729 natural *Caenorhabditis elegans* populations. *Genetics* 176: 999–1011.
- 730 Bates, D., M. Mächler, B. Bolker, and S. Walker, 2015 Fitting Linear Mixed-Effects  
731 Models Using *lme4*. *Journal of Statistical Software, Articles* 67: 1–48.
- 732 Berry, A. J., J. W. Ajioka, and M. Kreitman, 1991 Lack of polymorphism on the  
733 *Drosophila* fourth chromosome resulting from selection. *Genetics* 129: 1111–1117.
- 734 Boyd, W. A., M. V. Smith, and J. H. Freedman, 2012 *Caenorhabditis elegans* as a  
735 model in developmental toxicology. *Methods Mol. Biol.* 889: 15–24.
- 736 Braverman, J. M., R. R. Hudson, N. L. Kaplan, C. H. Langley, and W. Stephan, 1995  
737 The hitchhiking effect on the site frequency spectrum of DNA polymorphisms.  
738 *Genetics* 140: 783–796.
- 739 Brenner, S., 1974 The genetics of *Caenorhabditis elegans*. *Genetics* 77: 71–94.
- 740 Chang, C. C., C. C. Chow, L. C. Tellier, S. Vattikuti, S. M. Purcell *et al.*, 2015 Second-  
741 generation PLINK: rising to the challenge of larger and richer datasets. *Gigascience*  
742 4: 7.
- 743 Charlesworth, B., R. S. Singh, and M. K. Uyenoyama, 2003 The population genetics of  
744 life-history evolution. *The Evolution of Population Biology* 216–232.
- 745 Cook, D. E., S. Zdraljevic, J. P. Roberts, and E. C. Andersen, 2017 CeNDR, the  
746 *Caenorhabditis elegans* natural diversity resource. *Nucleic Acids Res.* 45: D650–  
747 D657.
- 748 Crombie, T. A., S. Zdraljevic, D. E. Cook, R. E. Tanny, S. C. Brady *et al.*, 2019 Deep  
749 sampling of Hawaiian *Caenorhabditis elegans* reveals high genetic diversity and  
750 admixture with global populations. *Elife* 8:e50465
- 751 Cutter, A. D., 2006 Nucleotide polymorphism and linkage disequilibrium in wild  
752 populations of the partial selfer *Caenorhabditis elegans*. *Genetics* 172: 171–184.
- 753 Cutter, A. D., 2004 Sperm-limited fecundity in nematodes: how many sperm are  
754 enough? *Evolution* 58: 651–655.
- 755 Endelman, J. B., 2011 Ridge regression and other kernels for genomic selection with R  
756 package rrBLUP. *Plant Genome* 4: 250–255.
- 757 Evans, K. S., and E. C. Andersen, 2020 The Gene *scb-1* Underlies Variation in

- 758        *Caenorhabditis elegans* Chemotherapeutic Responses. G3 10: 2353–2364.  
759        Evans, K. S., Y. Zhao, S. C. Brady, L. Long, P. T. McGrath *et al.*, 2017 Correlations of  
760        Genotype with Climate Parameters Suggest *Caenorhabditis elegans* Niche  
761        Adaptations. G3 7: 289–298.  
762        Fay, J. C., and C. I. Wu, 2000 Hitchhiking under positive Darwinian selection. Genetics  
763        155: 1405–1413.  
764        Félix, M.-A., and C. Braendle, 2010 The natural history of *Caenorhabditis elegans*. Curr.  
765        Biol. 20: R965–9.  
766        Félix, M.-A., and F. Duveau, 2012 Population dynamics and habitat sharing of natural  
767        populations of *Caenorhabditis elegans* and *C. briggsae*. BMC Biol. 10: 59.  
768        Flatt, T., 2020 Life-History Evolution and the Genetics of Fitness Components in  
769        *Drosophila melanogaster*. Genetics 214: 3–48.  
770        Flatt, T., and A. Heyland, 2011 *Mechanisms of Life History Evolution: The Genetics and*  
771        *Physiology of Life History Traits and Trade-Offs*. OUP Oxford.  
772        Frézal, L., and M.-A. Félix, 2015 *C. elegans* outside the Petri dish. Elife 4:e05849  
773        García-González, A. P., A. D. Ritter, S. Shrestha, E. C. Andersen, L. S. Yilmaz *et al.*,  
774        2017 Bacterial Metabolism Affects the *C. elegans* Response to Cancer  
775        Chemotherapeutics. Cell 169: 431–441.e8.  
776        Gilbert, K. J., S. Zdraljevic, D. E. Cook, A. D. Cutter, E. C. Andersen *et al.*, 2020 The  
777        distribution of mutational effects on fitness in *Caenorhabditis elegans* inferred from  
778        standing genetic variation. Cold Spring Harbor Laboratory 2020.10.26.355446.  
779        Hahnel, S. R., S. Zdraljevic, B. C. Rodriguez, Y. Zhao, P. T. McGrath *et al.*, 2018  
780        Extreme allelic heterogeneity at a *Caenorhabditis elegans* beta-tubulin locus  
781        explains natural resistance to benzimidazoles. PLoS Pathog. 14: e1007226.  
782        Hodgkin, J., and T. Doniach, 1997 Natural variation and copulatory plug formation in  
783        *Caenorhabditis elegans*. Genetics 146: 149–164.  
784        Houle, D., 1992 Comparing evolvability and variability of quantitative traits. Genetics  
785        130: 195–204.  
786        Kang, H. M., N. A. Zaitlen, C. M. Wade, A. Kirby, D. Heckerman *et al.*, 2008 Efficient  
787        control of population structure in model organism association mapping. Genetics  
788        178: 1709–1723.  
789        Kaplan, N. L., R. R. Hudson, and C. H. Langley, 1989 The “hitchhiking effect” revisited.  
790        Genetics 123: 887–899.  
791        Kim, Y., and R. Nielsen, 2004 Linkage disequilibrium as a signature of selective  
792        sweeps. Genetics 167: 1513–1524.  
793        Kiontke, K. C., M.-A. Félix, M. Ailion, M. V. Rockman, C. Braendle *et al.*, 2011 A  
794        phylogeny and molecular barcodes for *Caenorhabditis*, with numerous new species  
795        from rotting fruits. BMC Evol. Biol. 11: 339.  
796        Knight, G. R., and A. Robertson, 1957 Fitness as a Measurable Character in  
797        *Drosophila*. Genetics 42: 524–530.  
798        Lee, D., S. Zdraljevic, L. Stevens, Y. Wang, R. E. Tanny *et al.*, 2020 Balancing selection  
799        maintains ancient genetic diversity in *C. elegans*. Cold Spring Harbor Laboratory  
800        2020.07.23.218420.  
801        Li, H., 2011 A statistical framework for SNP calling, mutation discovery, association  
802        mapping and population genetical parameter estimation from sequencing data.  
803        Bioinformatics 27: 2987–2993.

- 804 McGrath, P. T., M. V. Rockman, M. Zimmer, H. Jang, E. Z. Macosko *et al.*, 2009  
805 Quantitative mapping of a digenic behavioral trait implicates globin variation in *C.*  
806 *elegans* sensory behaviors. *Neuron* 61: 692–699.  
807 Na, H., S. Zdraljevic, R. E. Tanny, A. J. M. Walhout, and E. C. Andersen, 2020 Natural  
808 variation in a glucuronosyltransferase modulates propionate sensitivity in a *C.*  
809 *elegans* propionic academia model. *PLoS Genet.* 16: e1008984.  
810 Ortiz, E. M., 2019 *vcf2phylip v2.0: convert a VCF matrix into several matrix formats for*  
811 *phylogenetic analysis.*  
812 Petersen, C., P. Dirksen, S. Prahl, E. A. Strathmann, and H. Schulenburg, 2014 The  
813 prevalence of *Caenorhabditis elegans* across 1.5 years in selected North German  
814 locations: the importance of substrate type, abiotic parameters, and *Caenorhabditis*  
815 competitors. *BMC Ecol.* 14: 4.  
816 Purcell, S., B. Neale, K. Todd-Brown, L. Thomas, M. A. R. Ferreira *et al.*, 2007 PLINK: a  
817 tool set for whole-genome association and population-based linkage analyses. *Am.*  
818 *J. Hum. Genet.* 81: 559–575.  
819 Richaud, A., G. Zhang, D. Lee, J. Lee, and M.-A. Félix, 2018 The Local Coexistence  
820 Pattern of Selfing Genotypes in *Caenorhabditis elegans* Natural Metapopulations.  
821 *Genetics* 208: 807–821.  
822 Rockman, M. V., and L. Kruglyak, 2009 Recombinational landscape and population  
823 genomics of *Caenorhabditis elegans*. *PLoS Genet.* 5: e1000419.  
824 Rockman, M. V., S. S. Skrovanek, and L. Kruglyak, 2010 Selection at linked sites  
825 shapes heritable phenotypic variation in *C. elegans*. *Science* 330: 372–376.  
826 Schliep, K. P., 2011 phangorn: phylogenetic analysis in R. *Bioinformatics* 27: 592–593.  
827 Schneider, C. A., W. S. Rasband, and K. W. Eliceiri, 2012 NIH Image to ImageJ: 25  
828 years of image analysis. *Nat. Methods* 9: 671–675.  
829 Shimko, T. C., and E. C. Andersen, 2014 COPASutils: an R package for reading,  
830 processing, and visualizing data from COPAS large-particle flow cytometers. *PLoS*  
831 *One* 9: e111090.  
832 Smith, J. M., and J. Haigh, 1974 The hitch-hiking effect of a favourable gene. *Genet.*  
833 *Res.* 23: 23–35.  
834 Stearns, S. C., 1976 Life-History Tactics: A Review of the Ideas. *Q. Rev. Biol.* 51: 3–47.  
835 Stearns, S. C., 1989 Trade-Offs in Life-History Evolution. *Funct. Ecol.* 3: 259–268.  
836 Stephan, W., 2019 Selective Sweeps. *Genetics* 211: 5–13.  
837 Stephan, W., Y. S. Song, and C. H. Langley, 2006 The hitchhiking effect on linkage  
838 disequilibrium between linked neutral loci. *Genetics* 172: 2647–2663.  
839 Stiernagle, T., 2006 Maintenance of *C. elegans*. *WormBook* 1–11.  
840 Ward, S., and J. S. Carrel, 1979 Fertilization and sperm competition in the nematode  
841 *Caenorhabditis elegans*. *Dev. Biol.* 73: 304–321.  
842 Wegewitz, V., H. Schulenburg, and A. Streit, 2008 Experimental insight into the  
843 proximate causes of male persistence variation among two strains of the  
844 androdioecious *Caenorhabditis elegans* (Nematoda). *BMC Ecol.* 8: 12.  
845 Yu, G., D. K. Smith, H. Zhu, Y. Guan, and T. T. Lam, 2017 Ggtree : An r package for  
846 visualization and annotation of phylogenetic trees with their covariates and other  
847 associated data. *Methods Ecol. Evol.* 8: 28–36.  
848 Zdraljevic, S., B. W. Fox, C. Strand, O. Panda, F. J. Tenjo *et al.*, 2019 Natural variation  
849 in *C. elegans* arsenic toxicity is explained by differences in branched chain amino

850 acid metabolism. Elife 8.:e40260